gratefully acknowledge the assistance of Andra Birkitt in preparing and operating the experiment.

References

[1]Morrisette, E. L., and Goldberg, T. J., "Turbulent-Flow Separation Criteria of Overexpanded Supersonic Nozzles," NASA Langley Research Center, NASA TP 1207, Hampton, VA, Aug. 1978.

[2]Murdock, J. W., and Welle, R. P., "Downstream Gas Effect on Nozzle Flow-Separation Location," AIAA Paper 99-2644, July 1999.

Adaptive Analysis of the Inviscid Supersonic Flow over a Backward-Facing Step

S. Y. Yang*
National Huwei Institute of Technology, Yunlin 632, Taiwan, Republic of China

Introduction

SEVERAL applications including scramjet, missile, rocket, and spacecraft may directly benefit from further understanding the supersonic flow over a backward-facing step. Research of flow separation and reattachment at supersonic speeds is commonly conducted in backward-facing step configurations. Such a flowfield can be described as a supersonic flow that turns beyond the step corner through an expansion fan and turns back to a direction approximately parallel to the inflow by an oblique reattachment shock wave. So far, numerous studies have been used to analyze supersonic backstep flows.[1–3] As mentioned by Venkatakrishnan,[4] unstructured grids provided flexibility for tessellating about complex geometry and for adapting to flow features, such as shocks. An underlying premise is that unstructured grid adaptation is far more automatable than are the tasks associated with multiblock structured grid generation. Recently, considerable effort has been made to develop solution-adaptive techniques[5–9] for solving the Euler/Navier–Stokes equations on unstructured meshes. By using the two-step Runge–Kutta Galerkin finite element method and a local remeshing technique,[5] a shock propagation within a channel was investigated. From the time-varying meshes directionally stretched elements were demonstrated. Webster et al.[6] developed an adaptive finite element methodology in which the finite quadtree mesh generator, interpolation-based error indicator, and edge-based mesh enrichment procedure were employed. On the quadrilateral-triangular mesh system Hwang and Fang[7] chose the magnitude of density gradient as an error indicator to perform the unsteady flow calculations, whereas Yang[8] took advantage of the absolute value of substantial derivative of Mach number as an error indicator to study oscillating cascade flows. The purpose of this work is to present a solution-adaptive solver to investigate the supersonic flow over a backward-facing step on mixed quadrilateral-triangular mesh. The Euler equations are solved in the Cartesian coordinate system. This solver includes the locally implicit scheme,[9] two-level refinement procedure,[7] and a modified error indicator.

Adaptive-Mesh Algorithm

The present adaptive algorithm includes the error indicator and two-level refinement technique. On quadrilateral-triangular meshes magnitude of density gradient[7] $|\nabla\rho|$ was employed as the error indicator to calculate the shock propagation in a channel, whereas the absolute value of substantial derivative of Mach number[8] $|DM/Dt|$ was chosen to capture the unsteady wave behavior and vortex-shedding phenomena. In the present calculations the steady solution is first achieved on the initial nonadaptive grid. According to the initial grid and steady solution, the adaptive mesh is accomplished using the error indicator and two-level refinement technique. Considering the supersonic flow over a backward-facing step, two mesh refinements are accomplished by choosing $|\nabla\rho|$ and $|\nabla M|$ as error indicators, respectively. It is found that neither of these two error indicators is capable of capturing the structure of the backstep corner vortex and expansion wave precisely. To capture the structure of the backstep corner vortex, the magnitude of gradient of vorticity magnitude $|\nabla\omega|$ ($\omega = |\nabla X \bar{V}|$, vorticity magnitude) is implemented as the error indicator to reperform the mesh refinement. According to the refined mesh, the structure of backstep corner vortex is captured clearly. However, it cannot capture the oblique shock and expansion wave behavior. Therefore, a modified error indicator is developed to capture the structure of backstep corner vortex, oblique shock wave, and expansion wave simultaneously. This modified error indicator EI can be written as follows:

$$EI = \frac{|\nabla P|}{|\nabla P|_{\max}} + \beta \frac{|\nabla\omega|}{|\nabla\omega|_{\max}} \tag{1}$$

where $|\nabla P|_{\max}$ and $|\nabla\omega|_{\max}$ are the maximum values of $|\nabla P|$ and $|\nabla\omega|$ among the computational cells. β represents the weighted coefficient and is chosen as 2.0. Because the order of magnitude of $|\nabla\omega|$ outnumbers that of $|\nabla P|$, it is essential to adjust both at the same order. Hence, $|\nabla P|$ and $|\nabla\omega|$ are divided by $|\nabla P|_{\max}$ and $|\nabla\omega|_{\max}$, respectively.

As for the two-level refinement technique, the value of EI of each unrefined cell is first calculated. The product of a specified constant C_1 and the average value of EI over the initial grid is selected as the first threshold value. If the value of EI of each unrefined cell is larger than the first threshold value C_1*$EIave$, the new node will be placed at the midpoint of each edge of quadrilateral/triangular cell or the center of quadrilateral cell.[7] After finishing the first-level refinement, the properties at all added new cells are interpolated from those at the initial grid. Continuing the second-level mesh refinement, the value of EI for each cell on the intermediate mesh and the corresponding second threshold value C_2*$EIave$ are computed. It is not necessary to perform any Euler iteration between level 1 and level 2 refinements. Normally, the value of constant C_2 is about two or three times bigger than that of constant C_1, and the value of constant C_1 ranges from 0.2 to 0.6. In the present calculation C_1 and C_2 are chosen as 0.4 and 1.0, respectively. Then the intermediate mesh is refined by reprocessing the first-level refinement technique. Because Webster et al.[6] mentioned that the mesh coarsening accounted for the majority of CPU cost during adaptation, the mesh coarsening procedure is not processed in this article.

Results and Discussion

The supersonic flow over a backward-facing step is investigated using the present solution algorithm. Geometric configuration and flowfield conditions are the same as those in the experiment.[2] Inlet Mach number, freestream temperature, freestream pressure, and velocity are set to 2.0, 167 K, 34.8 KPa, and 520 m/s, respectively. The averaged stagnation temperature and stagnation pressure measured in the experiment[2] were 310 K and 273 Kpa, respectively. The step height in the experiment was equal to 3.18 mm, whereas the width downstream of the backward-facing step was equal to 20.12 mm. The Mach 2 inlet flow expands through the centered Prandtl–Meyer expansion wave. A recirculation zone, which is essentially the backstep corner vortex, is formed behind the step and below the upper wall. Then the flow is turned back parallel to the upper wall and compressed through an oblique shock wave. The initial mesh shown in Fig. 1 incorporates the quadrilaterals and triangles, where the triangles are generated by the global remeshing algorithm.[5] This initial mesh may look like the multiblock grid with front quadrilaterals, intermediate triangles, and rear quadrilaterals,

Received 16 September 2000; revision received 24 February 2001; accepted for publication 23 March 2001.

*Associate Professor, Department of Aeronautical Engineering. Member AIAA.

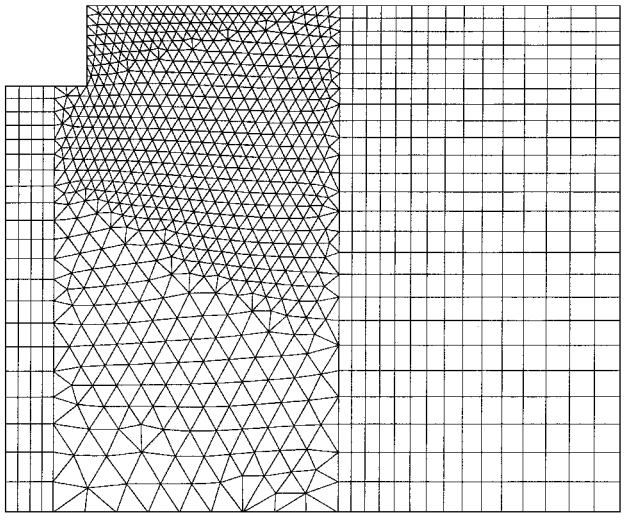

Fig. 1 Initial mesh of the supersonic flow over a backward-facing step (1746 cells).

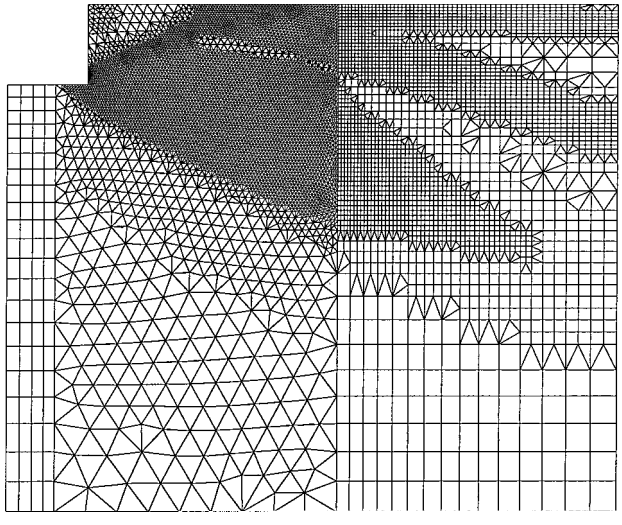

Fig. 2 Adaptive mesh obtained using $|\nabla \rho|$ as the error indicator (13118 cells).

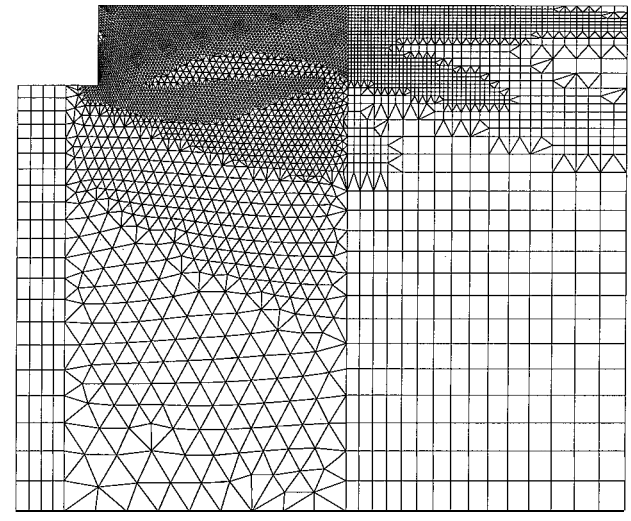

Fig. 3 Adaptive mesh obtained using $|\nabla M|$ as the error indicator (9459 cells).

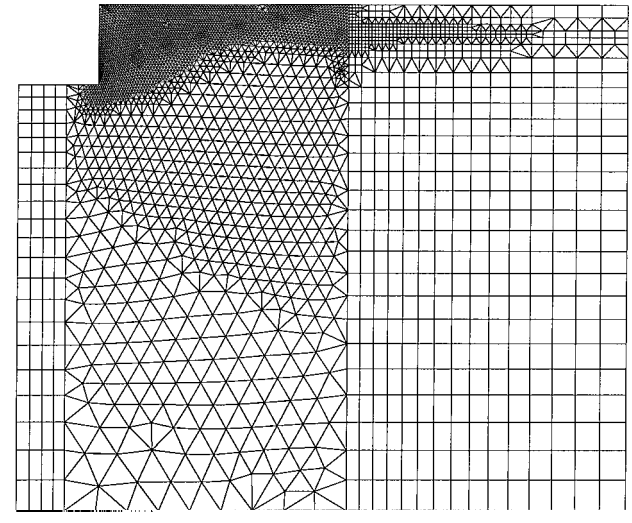

Fig. 4 Adaptive mesh obtained using $|\nabla \omega|$ as the error indicator (6688 cells).

in which two interfaces are encountered. Actually, the initial mesh is totally treated as a single unstructured mesh, and interfaces are removed. To promote the flowfield resolution, three error indicators $|\nabla\rho|$, $|\nabla M|$, and $|\nabla\omega|$ are carried out to refine the initial mesh respectively. The corresponding refined meshes are plotted in Figs. 2–4. Considering $|\nabla\rho|$ as an error indicator (see Fig. 2), the capability of capturing the structure of expansion wave and oblique shock wave is confirmed. However, it is unable to refine the backstep corner vortex. As for the refined mesh (see Fig. 3) obtained using $|\nabla M|$ as the error indicator, high-resolutional mesh is found inside the recirculation zone. The resolution is fair for the oblique shock wave, whereas it is poor for the expansion fan. Considering $|\nabla\omega|$ as an error indicator (see Fig. 4), the capability of capturing the backstep corner vortex is demonstrated. However, it is unable to capture the structure of expansion wave and oblique shock wave. To incorporate the advantages and avoid the disadvantages of the preceding three error indicators, a modified error indicator EI in Eq. (1) is developed in this work. From the refined mesh (see Fig. 5) obtained using this modified error indicator, the structure of backstep corner vortex, expansion wave, and oblique shock wave is clearly indicated. After achieving the steady solution on the refined mesh, the pressure contour is plotted in Fig. 6. To assess the accuracy of the present calculation, the pressure contour (see Fig. 6) is compared

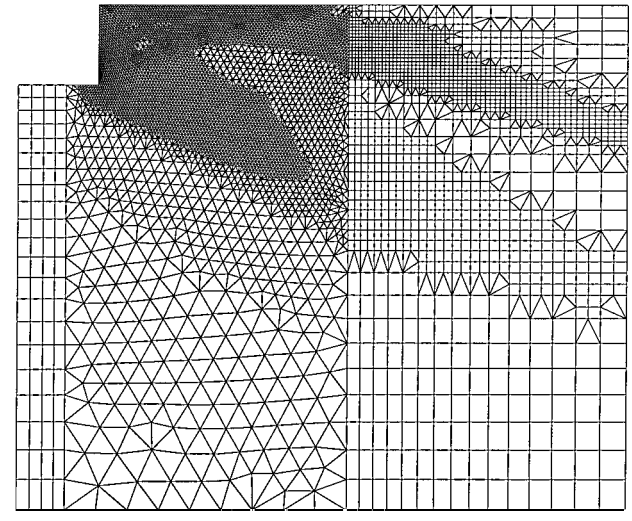

Fig. 5 Adaptive mesh obtained using the modified error indicator developed in the present paper (10781 cells).

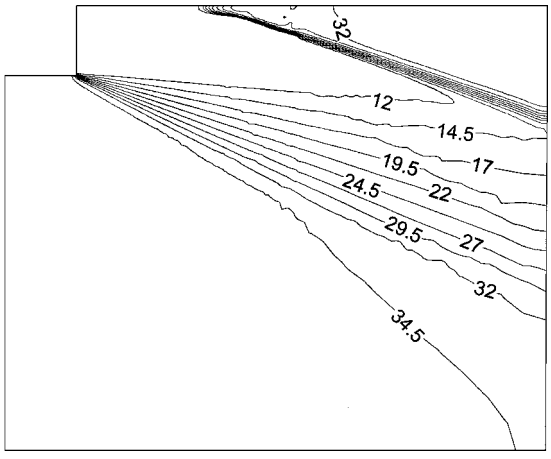

Fig. 6 Pressure contour obtained on the adaptive mesh Fig. 5.

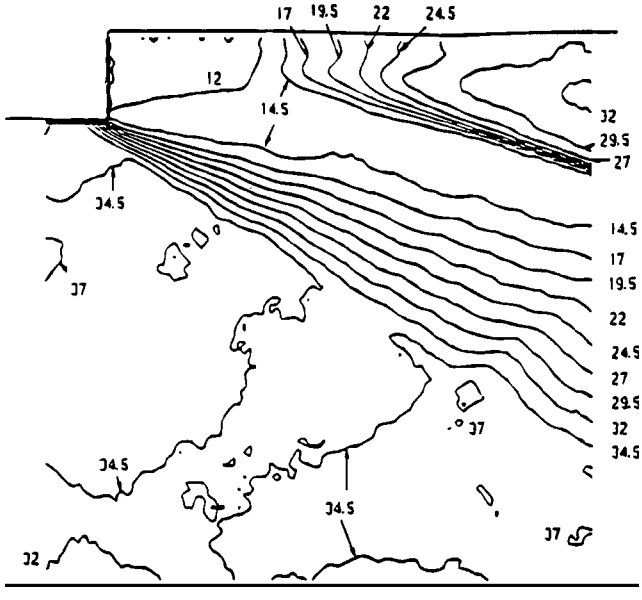

Fig. 7 Pressure contour obtained in the experiment.[2]

to that obtained in the experiment[2] (see Fig. 7). Based on the comparison, it is indicated that the present result can accurately capture the structure of Prandtl–Meyer expansion wave and oblique shock wave.

Conclusion

In the present work a solution-adaptive solver is presented to investigate the supersonic flow over a backward-facing step on mixed quadrilateral-triangular mesh. This solver incorporates the locally implicit scheme, two-level refinement procedure, and a modified error indicator. In a Cartesian coordinate system the Euler equations are solved. Based on the comparison of adaptive meshes obtained using four different error indicators, the modified error indicator can incorporate the advantages and avoid the disadvantages of the other three error indicators, which are $|\nabla\rho|$, $|\nabla M|$, and $|\nabla\omega|$. According to the adaptive mesh obtained using the modified error indicator, the structure of backstep corner vortex, expansion wave, and oblique shock wave is distinctly captured.

Acknowledgment

Support by the National Science Council of the Republic of China under Contract NSC 89-2212-E-150-016 is gratefully acknowledged.

References

[1]Loth, E., Kailasanath, K., and Lohner, R., "Supersonic Flow over an Axisymmetric Backward-Facing Step," *Journal of Spacecraft and Rockets*, Vol. 29, No. 3, 1992, pp. 352–359.

[2]Hartfield, R. J., Hollo, S. D., and McDaniel, J. C., "Planar Measurement Technique for Compressible Flows Using Laser Induced Iodine Fluorescence," *AIAA Journal*, Vol. 31, No. 3, 1993, pp. 483–490.

[3]Halupovich, Y., Natan, B., and Rom, J., "Numerical Solution of the Turbulent Supersonic Flow over a Backward Facing Step," *Fluid Dynamics Research*, Vol. 24, No. 5, 1999, pp. 251–273.

[4]Venkatakrishnan, V., "Perspective on Unstructured Grid Flow Solvers," *AIAA Journal*, Vol. 34, No. 3, 1996, pp. 533–547.

[5]Hwang, C. J., and Wu, S. J., "Global and Local Remeshing Algorithms for Compressible Flows," *Journal of Computational Physics*, Vol. 102, No. 1, 1992, pp. 98–113.

[6]Webster, B. E., Shephard, M. S., Rusak, Z., and Flaherty, J. E., "Automated Adaptive Time-Discontinuous Finite Element Method for Unsteady Compressible Airfoil Aerodynamics," *AIAA Journal*, Vol. 32, No. 4, 1994, pp. 748–757.

[7]Hwang, C. J., and Fang, J. M., "Solution-Adaptive Approach for Unsteady Flow Calculations on Quadrilateral-Triangular Meshes," *AIAA Journal*, Vol. 34, No. 4, 1996, pp. 851–853.

[8]Yang, S. Y., "Adaptive Analysis of Oscillating Cascade Flows on a Quadrilateral-Triangular Mesh," *Journal of Propulsion and Power*, Vol. 15, No. 3, 1999, pp. 479–481.

[9]Hwang, C. J., and Liu, J. L., "Inviscid and Viscous Solutions for Airfoil/Cascade Flows Using a Locally Implicit Algorithm on Adaptive Meshes," *Journal of Turbomachinery*, Vol. 113, No. 4, 1991, pp. 553–560.

Effect of Reynolds Number on Pitot-Pressure Distributions in Underexpanded Supersonic Freejets

Hiroshi Katanoda,* Taro Handa,† Yoshiaki Miyazato,‡
Mitsuharu Masuda,§ and Kazuyasu Matsuo¶
Kyushu University, Fukuoka 816-8580, Japan

Nomenclature

D	=	nozzle-exit diameter
e_{mean}	=	time-averaged output voltage of a hot-wire probe
e_{rms}	=	root-mean-squared output voltage of a hot-wire probe
p	=	pressure
p_i	=	pitot pressure
Re_d	=	Reynolds number based on the nozzle-exit condition
r	=	radial distance from jet centerline
r_m	=	Mach disk radius
x	=	axial distance from nozzle exit
x_m	=	Mach disk location

Subscripts

b	=	ambient condition
01	=	plenum chamber condition

Received 1 March 2000; revision received 26 February 2001; accepted for publication 16 March 2001.

*Postdoctoral Student, Department of Energy and Environmental Engineering, Graduate School of Engineering Sciences; currently Lecturer, Department of Mechanical Systems and Environmental Engineering, The University of Kitakyushu, 1-1 Hibikino, Wakamatsu-ku, Kitakyushu City; katanoda@env.kitakyu-u.ac.jp.

†Research Associate, Department of Energy and Environmental Engineering, Graduate School of Engineering Sciences, 6-1 Kasuga-Koen, Kasuga City; handa@ence.kyushu-u.ac.jp.

‡Associate Professor, Department of Energy and Environmental Engineering, Graduate School of Engineering Sciences, 6-1 Kasuga-Koen, Kasuga City; miyazato@ence.kyushu-u.ac.jp.

§Professor, Department of Energy and Environmental Engineering, Graduate School of Engineering Sciences, 6-1 Kasuga-Koen, Kasuga City; masuda@ence.kyushu-u.ac.jp.

¶Professor, Department of Energy and Environmental Engineering, Graduate School of Engineering Sciences, 6-1 Kasuga-Koen, Kasuga City; matsuo@ence.kyushu-u.ac.jp.